Matúš Tibenský; Angela Handlovičová

Two approaches for the approximation of the nonlinear smoothing term in the image segmentation

In: Karol Mikula (ed.): Proceedings of Equadiff 14, Conference on Differential Equations and Their Applications, Bratislava, July 24-28, 2017. Slovak University of Technology in Bratislava, SPEKTRUM STU Publishing, Bratislava, 2017. pp. 229–236.

Persistent URL: http://dml.cz/dmlcz/703062

Proceedings of EQUADIFF 2017
pp. 229–236

TWO APPROACHES FOR THE APPROXIMATION OF THE NONLINEAR SMOOTHING TERM IN THE IMAGE SEGMENTATION *

MATÚŠ TIBENSKÝ † AND ANGELA HANDLOVIČOVÁ ‡

Abstract. Purpose of the paper is to study nonlinear smoothing term initiated in [3], [4], [6] and [7] for problems of image segmentation and missing boundaries completion. The generalization of approach presented in [1] is proposed and applied in the field of image segmentation. So called regularised Riemannian mean curvature flow equation is studied and the construction of the numerical scheme based on the finite volume method approach is explained. The principle of the level set, for the first time given in [2], is used. We mention two different approaches for the approximation of the nonlinear smoothing term in the equation and known theoretical results for both of them. We provide the numerical tests for both schemes. It the last section we discuss obtained results and propose possibilities for the future research.

Key words. image segmentation, level set, regularised Riemannian mean curvature flow equation, finite volume method, approximation of the nonlinear smoothing term

1. Introduction. The main goal of the image segmentation is to divide given image to the parts called regions, to identify the pixels segmented object contains of or to add the boundary to the object, where it is missing. The errors we have to face with are mainly missing boundaries and noise. The range of application areas is wide and contains medicine, traffic control systems, recognition tasks and overall object detection and computer vision.

There are lot of techniques used in segmentation based on the various principles as statistical analysis, graph theory or machine learning. We are considering the approach based on the partial differential equations and especially so called level set methods based on the level set function introduced in [2].

2. Studied equation and assumptions on the data. We consider following problem arising in image segmentation as a generalisation of the approach given in [1], find an approximate solution to the equation

$$u_t - f_1(|\nabla u|)\nabla \cdot \left(g(|\nabla G_S * I^0|)\frac{\nabla u}{f(|\nabla u|)} \right) = r, \quad a.e.\ (x,t) \in \Omega \times (0,T). \tag{2.1}$$

Here the $u(x,t)$ is an unknown (segmentation) function defined in $Q_T \equiv [0,T] \times \Omega$, where Ω is bounded rectangular domain, $[0,T]$ is a time interval and I^0 is a given image, typically on this image is an object we want to segment.

We consider zero Dirichlet boundary condition

$$u = 0, \quad a.e.\ (x,t) \in \partial\Omega \times [0,T] \tag{2.2}$$

and initial condition

$$u(x,0) = u_0(x), \quad a.e.\ x \in \Omega. \tag{2.3}$$

*This work was supported by grants APVV 15-0522 and VEGA 1/0728/15.

†Dpt. of Mathematics, Slovak University of Technology in Bratislava, Radlinského 11, 810 05 Bratislava, Slovakia, (matus.tibensky@stuba.sk).

‡Dpt. of Mathematics, Slovak University of Technology in Bratislava, Radlinského 11, 810 05 Bratislava, Slovakia, (angela.handlovicova@stuba.sk).

The assumptions on the data in (2.1)-(2.3) are similar as in [1] and [3]. We can summarize them into the following hypothesis:

Hypothesis H

- (H1) Ω is a finite connected open subset of $\mathbb{R}^d$, $d \in \mathbb{N}$, with boundary $\partial\Omega$,
- (H2) $u_0 \in L^\infty(\Omega)$,
- (H3) $r \in L^2(\Omega \times (0,T))$ for all $T > 0$,
- (H4) $f \in C^0(\mathbb{R}_+; [a,b])$ is a Lipschitz continuous (non-strictly) increasing function, such that the function $x \mapsto x/f(x)$ is strictly increasing on $\mathbb{R}_+$. For practical application we are using $f(s) = \min(\sqrt{s^2+a^2}, b)$, where a and b are given positive parameters,
- (H5) $f_1 \in C^0(\mathbb{R}_+; [a_1, b_1])$, in general $a_1 \neq a$, $b_1 \neq b$, but for now in our model we consider the case $a_1 = a$ and $b_1 = b$,
- (H6) $g \in C^0(\mathbb{R}_+; [0,1])$ is decreasing function, $g(0) = 1$, $g(s) \to 0$ for $s \to \infty$. For practical numerical computation we use $g(s) = \frac{1}{1+Ks^2}$, where K is constant of sensitivity of function g and we choose it,
- (H7) $G_S \in C^\infty(\mathbb{R}^d)$ is a smoothing kernel (Gauss function), with width of the convolution mask S and such that $\int_{\mathbb{R}^d} G_S(x)dx = 1$, $\int_{\mathbb{R}^d} |G_S|dx \leq C_S, C_S \in \mathbb{R}$, $G_S(x) \to \delta_x$ for $S \to 0$, where δ_x is Dirac measure at point x and

$$(\nabla G_S * I^0)(x) = \int_{\mathbb{R}^d} \nabla G_S(x-\xi)\tilde{I^0}(\xi)d\xi, \tag{2.4}$$

where $\tilde{I^0}$ is extension of image I^0 to $\mathbb{R}^d$ given by periodic reflection through boundary of Ω and for which

$$1 \geq g^S(x) = g(|\nabla G_S * I^0|)(x) \geq \nu_S > 0 \tag{2.5}$$

for $\forall x \in \Omega$ due to properties of the convolution. The ν_S is a constant depending only on width of the convolution mask S.

Definition of the numerical scheme and the space discretisation of the equation we are generalising in this paper could be found in [1]. We apply method presented in [1] in the field of image segmentation, but in addition we have function g and convolution of the initial image with smoothing kernel in our approach (see [3] or [4]). For now just remark that discretisation of Ω, denoted by $\mathcal{D}$, is defined as the triplet $\mathcal{D} = (\mathcal{M}, \mathcal{E}, \mathcal{P})$, where $\mathcal{M}$ is a finite family of non-empty connected open disjoint subsets of Ω (the "control volumes") with measure marked by $|p|$, $\mathcal{E}$ is a finite family of disjoint subsets of $\overline{\Omega}$ (the "edges" of the mesh) with measure marked by $|\sigma|$ and $\mathcal{P}$ is a family of points of Ω indexed by $\mathcal{M}$, denoted by $\mathcal{P} = (x_p)_{p\in\mathcal{M}}$, such that for all $p \in \mathcal{M}$, $x_p \in p$ and p is assumed to be x_p-star-shaped so for all $x \in p$ the inclusion $[x_p, x] \subset p$ holds.

We say that $(\mathcal{D}, \tau)$ is a space-time discretisation of $\Omega \times (0,T)$ if $\mathcal{D}$ is a space discretisation of Ω in the sense we mentioned above and if there exists $N_T \in \mathbb{N}$ with $T = (N_T + 1)\tau$, where τ is a symbol for the time step.

Another important assumption on the discretisation we make is that

$$d_{p\sigma} n_{p,\sigma} = x_\sigma - x_p, \ \forall p \in \mathcal{M}, \ \forall \sigma \in \mathcal{E}_p, \tag{2.6}$$

where $\mathcal{E}_p$ denotes the set of the edges of the control volume p, $x_\sigma \in \sigma$, $d_{p\sigma}$ is a symbol for the Euclidean distance between x_p and hyperplane including σ (it is assumed that $d_{p\sigma} > 0$) and $n_{p,\sigma}$ denotes the unit vector normal to σ outward to p.

We define the set $H_{\mathcal{D}} \subset \mathbb{R}^{|\mathcal{M}|} \times \mathbb{R}^{|\mathcal{E}|}$ such that $u_\sigma = 0$ for all $\sigma \in \mathcal{E}_{\text{ext}}$ (the set of boundary interfaces). We define the following functions on $H_{\mathcal{D}}$:

$$N_p(u)^2 = \frac{1}{|p|} \sum_{\sigma \in \mathcal{E}_p} \frac{|\sigma|}{d_{p\sigma}} (u_\sigma - u_p)^2, \ \forall p \in \mathcal{M}, \ \forall u \in H_{\mathcal{D}}, \tag{2.7}$$

where u_p is defined as $u_p = u(x_p)$ and u_σ is defined as $u_\sigma = u(x_\sigma)$.

Let us recall that

$$\|u\|_{1,\mathcal{D}}^2 = \sum_{p \in \mathcal{M}} |p| N_p(u)^2 \tag{2.8}$$

defines a norm on $H_{\mathcal{D}}$ (see [1] and references there).

Under the above mentioned assumptions and notations the semi-implicit scheme is defined by

$$u_p^0 = u_0(x_p), \ \forall p \in \mathcal{M}, \tag{2.9}$$

$$u_\sigma^0 = u_0(x_\sigma), \ \forall \sigma \in \mathcal{E}, \tag{2.10}$$

$$r_p^{n+1} = \int_{n\tau}^{(n+1)\tau} \int_p r(x,t) dx dt, \ \forall p \in \mathcal{M}, \ \forall n \in \mathbb{N}, \tag{2.11}$$

$$u_\sigma^{n+1} = 0, \ \forall \sigma \in \mathcal{E}_{\text{ext}}, \ \forall n \in \mathbb{N}, \tag{2.12}$$

and

$$\begin{aligned} &\frac{|p|}{\tau \ f_1(N_p(u^n))}(u_p^{n+1} - u_p^n) - \frac{1}{f(N_p(u^n))} \sum_{\sigma \in \mathcal{E}_p} g_{\mathcal{D}}^S \frac{|\sigma|}{d_{p\sigma}} (u_\sigma^{n+1} - u_p^{n+1}) = \\ &\quad = \frac{r_p^{n+1}}{\tau \ f_1(N_p(u^n))}, \forall p \in \mathcal{M}, \ \forall n \in \mathbb{N}, \end{aligned} \tag{2.13}$$

where the following relation is given for the interior edges

$$\frac{u_\sigma^{n+1} - u_p^{n+1}}{f(N_p(u^n)) \ d_{p\sigma}} + \frac{u_\sigma^{n+1} - u_q^{n+1}}{f(N_q(u^n)) \ d_{q\sigma}} = 0, \tag{2.14}$$

$\forall n \in \mathbb{N}$, $\forall \sigma \in \mathcal{E}_{\text{int}}$ (the set of interior interfaces) where σ is the edge between p and q.

For the explanation of the selection of u_p^0 and u_σ^0, which impacts the assumptions given on function u_0 in (H2) see [8].

There are two options how to choose $g_{\mathcal{D}}^S$ (approximation of g^S) in (2.13) considered in this paper. First one, we will label it **(APR1)**, is for $\forall \sigma \in \mathcal{E}$ defined by

$$g_\sigma^S := g^S(x_\sigma) = g(|\int_{\mathbb{R}^d} \nabla G_S(x_\sigma - \xi) \tilde{I^0}(\xi) d\xi|). \tag{2.15}$$

It means that the convolution of the initial image with Gaussian kernel is done in the points x_σ on the border of the control volume, which is exactly the point where it, from (2.13), should be done.

The second one, labeled as **(APR2)**, is $\forall p \in \mathcal{M}$ defined by

$$g_p^S := g^S(x_p) = g(|\int_{\mathbb{R}^d} \nabla G_S(x_p - \xi) \tilde{I^0}(\xi) d\xi|). \tag{2.16}$$

This means that the convolution is done in the points x_p inside the control volume, so we are making an error. The problem we are interested in is the impact of this approximation error on the final model and it segmentation ability.

3. Theoretical results. Theoretical properties for the scheme (2.13) - (2.14) with the approximation **(APR2)** as the stability estimates on the numerical solution, the uniqueness of the numerical solution, the convergence of the numerical scheme to the weak solution and the convergence of the approximation of the numerical gradient were proven in [5].

For the approximation **(APR1)** the case is more complex and the stability of the scheme is conditional, the time step and the space step have to be the same order to guarantee the stability estimates on the numerical solution and all of the other theoretical features mentioned above.

If we summarize, from the perspective of the theory the approximation **(APR2)** is better as we are able to prove unconditional stability for the scheme (2.13) - (2.14). On the other hand with this choice of approximation we are making bigger approximation error than for **(APR1)**. How big impact does this error have on the computations we test in the next section.

4. Numerical experiments. For testing of the difference between **(APR1)** and **(APR2)** we chose following benchmark example (see Figure 4.1) - noised square with missing boundaries as an example of the object with both typical errors occuring in the image segmentation - noise and missing boundaries. On the other hand with square as an simple object we know the desired shape of the level function, so we can test accuracy and speed of the approximations even without knowing the exact solution of the problem.

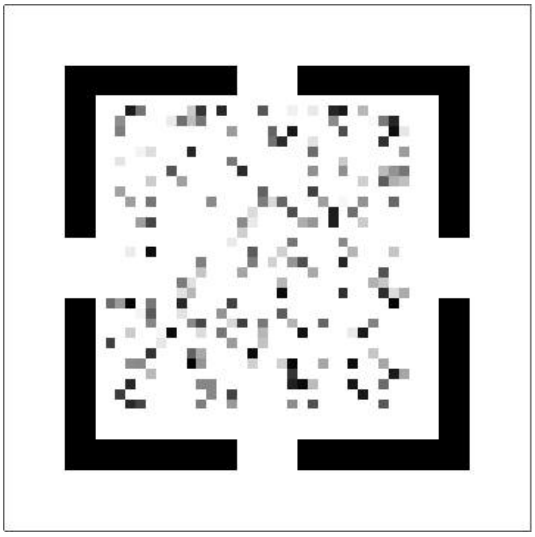

FIG. 4.1. *Object we want to segment.*

The approach we are presenting in this paper is based on the idea of the level set function. At the beginning of the segmentation process we construct initial level set function (Figure 4.2), which is developing in the time by the mean curvature and the constructed vector field tends the level set function to the border of the segmented object. Instead of creating developing curve to segment the object, we create the level set function and we monitor the development of the segmented area implicitly by looking on its isolines. This type of approach is robust against topological changes.

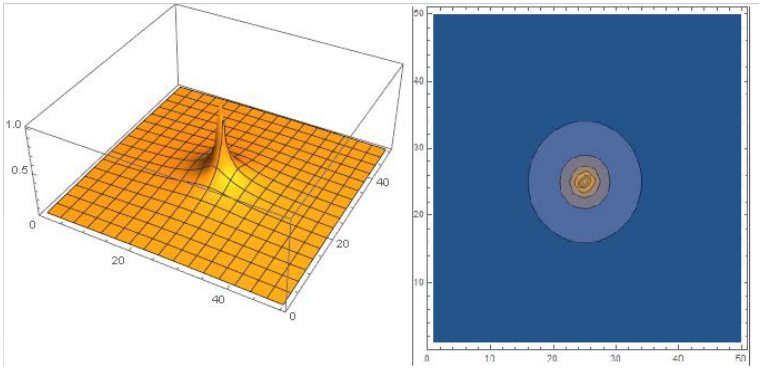

FIG. 4.2. *Initial level set function.*

4.1. Visual test. As the first comparison of the different choices of approximation of nonlinear smoothing term in (1) we chose the visual test.

We can take a look on the difference that made two different approximation on the initial image (see Figure 4.3). The difference is defined as model with **(APR2)** minus model with **(APR1)**. One can see that **(APR2)** is better in presmoothing of the noise in the image, but, on the other hand, the borders of the object are little bit more blurry.

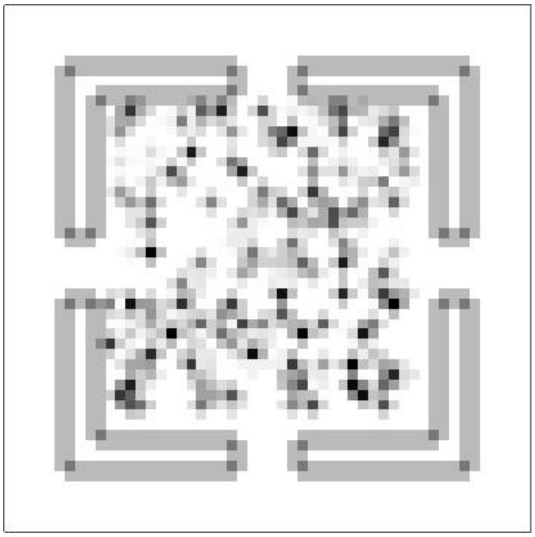

FIG. 4.3. *Difference for the initial image.*

This is the graphical impact of the choice of the approximation. Now take a look on the difference between level set functions in the various time steps. On the Figure 4.4 we can see that the difference in the time very slightly increase, but even after 1000 time steps, when the object is segmented the difference is still less than 0.001 in absolute numbers. So from graphical perspective it seems that the **(APR1)** is slightly better, but the difference is small. To make these initial observations more precise we do the numerical tests as well.

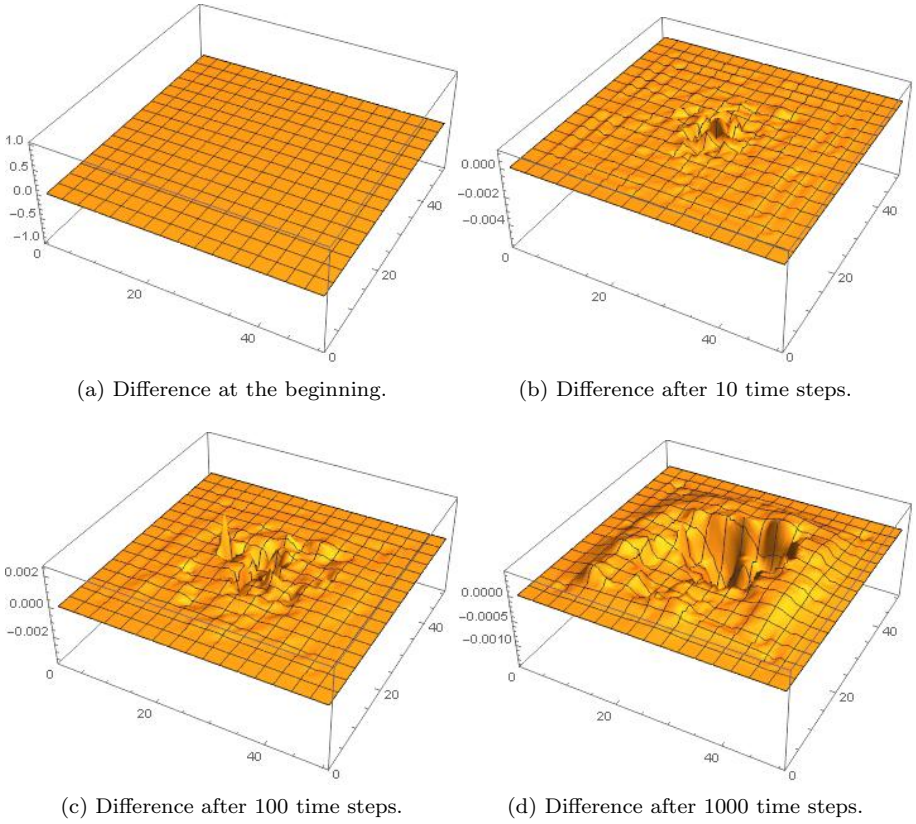

(a) Difference at the beginning.

(b) Difference after 10 time steps.

(c) Difference after 100 time steps.

(d) Difference after 1000 time steps.

FIG. 4.4. *Difference between level set functions.*

4.2. Numerical comparison. The second comparison of approximation of nonlinear smoothing term in (1) we are presenting in this paper are the absolute and relative L_1, L_2 and L_∞ norms of the difference between the segmentation level set functions:

TABLE 4.1
Absolute and relative norms for sensitivity constant $K = 1$.

Absolute difference after	1 step	10 steps	100 steps	1000 steps
L_1 norm	0.00612	0.13982	0.22316	0.29966
L_2 norm	0.00001	0.00004	0.00013	0.00009
L_∞ norm	0.00086	0.00244	0.00309	0.00098
Relative difference after	1 step	10 steps	100 steps	1000 steps
L_1 norm	0.00039	0.00091	0.00151	0.00098
L_2 norm	7.53e-08	2.78e-07	8.79e-07	7.20e-07
L_∞ norm	5.53e-06	1.59e-05	2.09e-05	7.44e-06

From these numbers we are able to conclude the same result as from the visual test - the difference between model with **(APR1)** and model with **(APR2)** is too small to make any relevant impact on the final result of segmentation (biggest relative error is less than 0.2 %).

There is one more parameter that can make an impact - constant K, the constant of sensitivity of the function g mentioned in (H6). In the first example above we set $K = 1$, so lets increase this value and check if it has a significant impact.

In the next table we list L_1, L_2 and L_∞ norms of the absolute and relative difference between the segmentation level set functions for sensitivity constant $K = 10$:

TABLE 4.2
Absolute and relative norms for sensitivity constant K = 10.

Absolute difference after	1 step	10 steps	100 steps	1000 steps
L_1 norm	0.03299	0.10126	0.18812	0.16514
L_2 norm	0.00001	0.00001	0.00008	0.00002
L_∞ norm	0.00082	0.00304	0.00158	0.00021
Relative difference after	1 step	10 steps	100 steps	1000 steps
L_1 norm	0.00021	0.00067	0.00133	0.00161
L_2 norm	5.22e-08	3.88e-07	5.88e-07	2.01e-07
L_∞ norm	5.29e-06	2.01e-05	1.11e-05	2.06e-06

Comparing these numbers with the ones from Table 4.1 one can see that the choice of the constant K do not play a big role in overall process of the segmentation when looking on the difference between segmantation level set functions.

5. Conclusion. In this paper we pay attention on the options of approximation of the nonlinear smoothing term in the image segmentation. We compared both approaches from theoretical and numerical perspective.

In the Section 3 we mention that model with **(APR2)** has better theoretical features, especially the stability of the scheme and convergence is unconditional compared to conditional stability and convergence of the semi-implicit shceme for model with **(APR1)**, here the time step and the space step have to be the same order.

Section 4 was dedicated to numerical comparison of both models. Overall result is that from numerical perspective is better the model with **(APR1)**, but the difference and impact of choice of the approximation is minimal and not significant.

Overall is seems more reasonable to use **(APR2)** as it is easier for implimentation, there is a proof of all needed theoretical aspects of the model and the difference in numerical computation is negligible.

For the future research we plan to study and evaluate the importance of the nonlinear smoothing term in the image segmentation overall.

REFERENCES

[1] Eymard R., Handlovičová A., Mikula K.: Study of a finite volume scheme for regularised mean curvature flow level set equation, IMA Journal on Numerical Analysis, Vol. 31, 813-846, 2011.
[2] Osher S., Sethian J. A.: Fronts propagating with curvature-dependent speed: Algorithms based on Hamilton-Jacobi formulations, J. Comput. Phys., 79(1):12-49, 1988.
[3] Mikula K., Sarti A., Sgallarri A.: Co-volume method for Riemannian mean curvature flow in subjective surfaces multiscale segmentation, Computing and Visualization in Science, Vol. 9, No. 1, 23-31, 2006.
[4] Mikula K., Sarti A., Sgallari F.: Co-volume level set method in subjective surface based medical image segmentation, in: Handbook of Medical Image Analysis: Segmentation and Registration Models (J.Suri et al., Eds.), Springer, New York, 583-626, 2005.
[5] Handlovičová A., Tibenský M.: Convergence of the numerical scheme for regularised Riemannian

mean curvature flow equation, submitted to Tatra Mountains Mathematical Publications, 2017.
[6] Mikula K., Ramarosy N.: Semi-implicit finite volume scheme for solving nonlinear diffusion equations in image processing, Numerische Mathematik 89, No. 3, 561-590, 2001.
[7] Tibenský M.: Využitie metód založených na level set rovnici v spracovaní obrazu, Faculty of mathematics, physics and informatics, Comenius University, 2016.
[8] Droniou J., Nataraj N.: Improved L^2 estimate for gradient schemes, and super-convergence of the TPFA finite volume scheme, IMA Journal of Numerical Analysis 2017, 2016.